International Journal of Pharmaceutics 377 (2009) 76–84

Contents lists available at ScienceDirect

International Journal of Pharmaceutics

journal homepage: www.elsevier.com/locate/ijpharm

Chitosan–phospholipid blend for sustained and localized delivery of docetaxel to the peritoneal cavity

Payam Zahedi[a], Raquel De Souza[a], Micheline Piquette-Miller[a], Christine Allen[a,b,*]

[a] Department of Pharmaceutical Sciences, Leslie Dan Faculty of Pharmacy, University of Toronto, 144 College Street, Toronto, Ontario, Canada M5S 3M2
[b] Department of Chemistry, Faculty of Arts and Science, University of Toronto, 80 St. George Street, Toronto, Ontario, Canada M5S 3H6

ARTICLE INFO

Article history:
Received 27 April 2009
Accepted 3 May 2009
Available online 12 May 2009

Keywords:
Chitosan
Docetaxel
Injectable
Intraperitoneal
Localized sustained delivery
Phospholipid

ABSTRACT

Localized and sustained delivery of chemotherapeutics presents a "magic bullet" effect by providing high drug concentrations at the target site, extended drug exposure and reduced systemic toxicity. In the present study, an injectable chitosan–phospholipid ($PoLi_{gel}$) blend is put forth as a strategy to achieve sustained and localized delivery of docetaxel (DTX) following intraperitoneal (IP) administration. The stability of the blend was confirmed *in vitro*, by turbidity measurements and attributed to specific molecular interactions and the organization of the materials within the blend, as evidenced by FTIR analysis and confocal laser scanning microscopy, respectively. The chitosan and phospholipid were found to colocalize in regions surrounding a mean object area of 11.2 μm^2 with colocalization coefficients of 43% and 46% for the chitosan and phospholipid, respectively. The $PoLi_{gel}$ blend afforded sustained drug release as seen both *in vitro* (2.4 ± 0.7% DTX per day) and *in vivo* (4.4 ± 0.7% DTX per day). Constant concentrations of DTX were observed over a 2-week period in plasma and relevant peritoneal tissues, with no signs of toxicity or inflammation, following IP administration of the blend in healthy CD-1 mice. At DTX doses of 28.8 and 19.2 mg/kg, the blend showed significant tumor inhibition of 87.3 ± 9.3% and 74.1 ± 25.9%, respectively, in a murine xenograft model of human ovarian adenocarcinoma. This localized delivery system has shown excellent potential for sustained IP treatment of cancers, such as ovarian, that reside in the peritoneal cavity.

1. Introduction

Traditionally chemotherapy has consisted of systemic, intermittent administration at the maximum tolerated dose, yet this can lead to acute and long-term toxicities (Lowenthal and Eaton, 1996; Kerbel and Kamen, 2004), inadequate dosing at the target site (Fung and Saltzman, 1997; Gottesman, 2002; Tannock et al., 2002), and development of drug resistance (Gottesman, 2002; Kerbel, 2005). Localized delivery of lower doses of chemotherapy in a sustained manner presents a "magic bullet" effect by providing high drug concentrations at the target site, extended drug exposure which may be particularly beneficial for cell cycle specific drugs, and lower systemic toxicity (Dhanikula and Panchagnula, 1999; Kerbel and Kamen, 2004). Implantable and injectable systems including polymer-based injectable pastes, gels, microspheres and nanospheres have been pursued for localized cancer therapy (Fung and Saltzman, 1997; Hatefi and Amsden, 2002; Parveen and Sahoo, 2008; Ta et al., 2008). However, the majority of these systems are derived from polyester-based polymers (Dhanikula and Panchagnula, 1999; Sinha and Trehan, 2005; Tsai et al., 2007; Vukelja et al., 2007), which are known to produce a foreign body response (i.e. fibrous encapsulation) and acidic by-products that can accelerate drug degradation (Hickey et al., 2002; Fulzele et al., 2003; Grayson et al., 2004; Ho et al., 2005). As a result, there has been an increased interest in the use of naturally occurring polymers such as protein-based polymers (e.g. collagen and gelatin) and polysaccharides (e.g. chitosan and agarose) to alleviate the issues associated with polyester systems (Angelova and Hunkeler, 1999; Pillai and Panchagnula, 2001).

Paclitaxel (PTX) and its semi-synthetic analogue docetaxel (DTX), two FDA approved taxanes, show considerable activity in the treatment of breast, lung and ovarian cancers (Crown and O'Leary, 2000). PTX and DTX are highly lipophilic with reported water solubilities of 0.3 and 5–6 μg/ml, respectively (Ali et al., 1997). For this reason, the non-ionic surfactants Cremophor EL and polysorbate 80 are currently used as formulation vehicles for PTX (Taxol®, Bristol-Myers Squibb) and DTX (Taxotere®, Sanofi-Aventis), respectively. These surfactants have been associated with hypersensitivity and neurotoxicity, and have been shown to alter cellular uptake and influence drug distribution (van Zuylen et al., 2001; Hennenfent

* Corresponding author at: Leslie Dan Faculty of Pharmacy, University of Toronto, 144 College Street, Toronto, Ontario, Canada M5S 3M2. Tel.: +1 416 946 8594; fax: +1 416 978 8511.
E-mail address: cj.allen@utoronto.ca (C. Allen).

0378-5173/$ – see front matter © 2009 Elsevier B.V. All rights reserved.
doi:10.1016/j.ijpharm.2009.05.003

and Govindan, 2006; Engels et al., 2007). Alternative strategies have been explored for surfactant-free delivery of taxanes in order to circumvent these toxicity issues (Panchagnula, 1998; Engels et al., 2007). As an example, our group developed an implantable chitosan–phospholipid film for localized, sustained delivery of PTX in the peritoneal cavity (Grant et al., 2005). *In vitro* studies in an ovarian carcinoma cell line and *in vivo* studies in both healthy mice and a murine xenograft model of human ovarian cancer have confirmed that the chitosan-based films are biocompatible, non-immunogenic, non-toxic, efficacious and provide a sustained release of PTX over periods of up to 4 months (Grant et al., 2005, 2007; Ho et al., 2005, 2007; Vassileva et al., 2007, 2008b; Lim Soo et al., 2008). Due to the invasive nature of surgical implantation, an injectable formulation with similar functional attributes and improved ease of administration was pursued for PTX (Grant et al., 2008).

It has been shown that DTX is more effective than PTX in a number of preclinical and clinical investigations due to improved cellular uptake and lower efflux, increased potency, lower incidence of neurotoxicity and increased efficacy in PTX-resistant disease (Clarke and Rivory, 1999; Maenpaa, 2003; Gligorov and Lotz, 2004). Furthermore, to date no localized and sustained delivery systems for DTX have been reported. In the present study, the physicochemical and rheological properties as well as *in vivo* performance of an injectable chitosan–phospholipid blend were evaluated as a formulation strategy for intraperitoneal (IP) sustained delivery of DTX.

2. Materials and methods

2.1. Materials

Chitosan (MW ~ 202 kDa, 94.5% degree of deacetylation) was purchased from Marinard Biotech Inc. (Quebec City, Canada). Anhydrous docetaxel (98%) was purchased from Lianyungang Jari Pharmaceutical Co. (Jiangsu, China). Egg phosphatidylcholine (ePC), glycidyltrimethylammonium chloride (GTMAC), C12 lauric chloride (LCl), and C12 lauric aldehyde (LA) were purchased from Sigma–Aldrich Chemical Co. (Oakville, Canada) and used without further purification. The fluorescent probes, Alexa Fluor® 633 and 1,2-dipalmitoyl-sn-glycero-3-phosphoethanolamine-N-(7-nitro-2-1,3-benzoxadiazol-4-yl) (NBD-DPPE) were purchased from Molecular Probes Inc. (Eugene, USA) and Avanti Polar Lipids Inc. (Alabaster, USA), respectively. SKOV3 human ovarian adenocarcinoma cell line was obtained from the American Type Culture Collection (Rockville, USA). RPMI 1640 cell culture medium was purchased from Gibco (Grand Island, USA). Fetal bovine serum and penicillin–streptomycin were purchased from Invitrogen (Burlington, Canada). All other chemicals were reagent grade and used as received.

2.2. Chitosan–phospholipid blend preparation

A water-soluble chitosan (WSC) derivative was synthesized using a method reported previously (Cho et al., 2006). Briefly, chitosan was suspended in a 0.5% (v/v) acetic acid solution, and GTMAC was added dropwise (GTMAC:chitosan 3:1, mol/mol). The reaction was stirred at 55 °C for 18 h. Following the reaction, undissolved chitosan was removed by centrifugation of the reaction mixture at 5000 rpm for 10 min at 25 °C (Centrifuge 5804T, Eppendorf, Germany). Excess GTMAC was removed using methanol followed by precipitation of the WSC in acetone. This procedure was repeated in triplicate and the purified WSC was dried in a vacuum oven at 25 °C with subsequent grinding of the product to obtain a fine powder. FTIR analysis and ^{1}H NMR spectra were used to confirm the conjugation of GTMAC to chitosan (data not shown) (Cho et al., 2006). The degree of substitution of GTMAC on the chitosan backbone was calculated to be 45% using an established titration method (Lim and Hudson, 2004).

Chitosan–phospholipid ($PoLi_{gel}$) blends were prepared as outlined elsewhere (Grant et al., 2008). In brief, WSC was dissolved in distilled deionized water to prepare a 4.2% (w/v) solution. ePC was solubilized in LA or LCl (ePC to LA or LCl ratio of 1:4, w/w) and then added to the WSC solution. The final material ratio of the WSC–LA–ePC ($PoLi_{gel}$–LA) or WSC–LCl–ePC ($PoLi_{gel}$–LCl) blends was 1:4:1 (w/w/w). For preparation of drug-loaded blends, firstly DTX (10, 20 and 30 mg) dissolved in anhydrous ethanol was dried under nitrogen to form a thin-layered film and then placed under vacuum for 24 h to remove any residual solvent. An ePC–LA solution was used to re-suspend the DTX film prior to mixing with WSC solution to achieve WSC–LA–ePC–DTX ($PoLi_{gel}$–LA–DTX) blends with final material ratios of 1:4:1:(DTX: 0.24, 0.48 and 0.71) (w/w/w/w).

2.3. Characterization of $PoLi_{gel}$ blend stability and pH profile

The stability and pH profile of $PoLi_{gel}$–LA, $PoLi_{gel}$–LA–DTX (1:4:1:0.71, w/w/w/w) and $PoLi_{gel}$–LCl blends were assessed in buffer solution containing lysozyme stored at 37 °C over a 2-week period, as outlined elsewhere with slight modifications (Grant et al., 2008). 150 μl of each blend was injected into a vial containing 15 ml 0.01 M PBS (pH 7.4) and 2 mg/ml lysozyme. At specific time points, an aliquot was removed for stability and pH measurements, and then returned to the vial containing the blend for subsequent analysis. For stability assessment, turbidity analysis was conducted using a UV spectrophotometer with λ = 700 nm (Cary 50 UV–vis spectrophotometer, Varian Inc., USA). pH was measured under constant stirring by a pH meter (SympHony SB20 pH meter, VWR Scientific, USA).

2.4. Fourier transform infrared spectroscopy analysis

Fourier transform infrared (FTIR) spectra of the $PoLi_{gel}$–LA and $PoLi_{gel}$–LCl blends and their individual components were obtained using a universal ATR Spectrum-one spectrophotometer (Spectrum One FTIR, Perkin-Elmer, USA). The spectra were recorded from 4000 to 650 cm^{-1} and analyzed using Spectrum V5.0.1 software (Perkin-Elmer, USA). All spectra were an average of 20 scans at a resolution of 2 cm^{-1} and repeated in triplicate.

2.5. Confocal microscopy analysis

The $PoLi_{gel}$–LA blend was analyzed using an inverted two photon confocal laser scanning fluorescence microscope (LSM 510 META, Carl Zeiss MicroImaging Inc., Germany) as outlined elsewhere (Grant et al., 2008). In brief, the fluorescent probe Alexa Fluor® 633 (λ_{ex} = 632 nm, λ_{em} = 647 nm), which contains an amine reactive group, was conjugated to the WSC according to the manufacturer's protocol and quantified by FTIR analysis (data not shown). To prepare the fluorescent-labeled $PoLi_{gel}$–LA, 1 mol% of the fluorescent phospholipid NBD-DPPE (λ_{ex} = 460 nm, λ_{em} = 534 nm) was mixed with an ePC–LA solution. The ePC–LA fluorescent solution was then mixed with WSC solution containing 1% (w/w) of the Alexa Fluor® 633 conjugated WSC to prepare a final WSC–ePC–LA 1:4:1 (w/w/w) fluorescent blend. The fluorescent blend was cast onto a glass slide, covered with a glass cover slip and allowed to dry in the dark for 24 h prior to microscopy analysis. A colocalization map was generated from the images obtained. Parameters including colocalization coefficients, mean object area, and mean gray value were obtained by Image-Pro Analyzer V6.3 (Media Cybernetics Inc, USA).

2.6. Rheological measurements

The rheological properties of the $PoLi_{gel}$–LA, $PoLi_{gel}$–LA–DTX and $PoLi_{gel}$–LCl blends were characterized by a stress-controlled rheometer with a 4 cm cone and 2° angle plate geometry attachment at room temperature (AR-2000, TA Instruments, USA). The rheometer was calibrated and rotational mapping was performed according to instrument specifications. The viscosity was measured using a continuous ramping flow mode while increasing the shear stress from 1 to 500 Pa. The blends were stored for 3 h prior to mechanical testing. A 600 μl injection of each sample was placed on the rheometer plate for testing.

2.7. In vitro DTX release

$PoLi_{gel}$–LA–DTX blends of different initial DTX loading levels (WSC–LA–ePC–DTX material ratios: 1:4:1:(0.24, 0.48 and 0.71), w/w/w/w) were injected into vials containing 15 ml of 0.01 M PBS (pH 7.4) with 2 mg/ml lysozyme and 40 mg/ml albumin. The samples were incubated at 37 °C and at specific time points 12 ml aliquots were removed for analysis by high-performance liquid chromatography (HPLC). The removed volume was replaced with 12 ml fresh 0.01 M PBS (pH 7.4) containing 2 mg/ml lysozyme and 40 mg/ml albumin.

2.8. In vivo characterization

In vivo studies were conducted in healthy female CD-1 mice (6–8 weeks old, 20–25 g) purchased from Charles River (St. Constant, Canada). All studies were conducted in accordance with the guidelines of the University of Toronto Animal Care Committee and the Canadian Animal Care Council. Each mouse was injected IP with 30 μl $PoLi_{gel}$–LA–DTX (total DTX dose: 28.8 mg/kg) blend in the lower left quadrant, with an injection depth of 1 cm using a 25-gauge needle. The 28.8 mg/kg dose was chosen as it corresponds to the clinically relevant IP DTX dose given as Taxotere® in humans (Morgan et al., 2003). Samples were sterilized under UV-light (Sterilizer T209, Intercosmetics, Canada) for 3 h prior to injection. Mice were weighed and observed weekly for signs of distress (e.g. weight loss, paleness, and inactivity). Control mice did not receive an injection. At specific time points, mice ($n = 6$) were anesthetized and sacrificed by exsanguinations via cardiac puncture. Plasma and relevant peritoneal tissues were collected for HPLC analysis.

Animals were assessed daily throughout the study for signs of DTX toxicity, infection at injection site, peritonitis and weight loss. The peritoneal cavity was assessed post mortem for signs of fibrous encapsulation and inflammation. Hepatotoxicity was assessed by alanine aminotransferase (ALT) activity in serum using an ALT (GTP) Reagent kit (Thermo Electron Corporation, Australia) following the manufacturer's protocol. Systemic inflammation was assessed by measuring levels of circulating interleukin-6 (IL-6) using a mouse IL-6 ELISA kit according to manufacturer's instructions (BD Biosciences, USA).

2.9. In vivo efficacy assessment

Efficacy studies were conducted in female CD-1 nu/nu mice (6–8 weeks old, 18–20 g) purchased from Charles River (St. Constant, Canada). All studies were conducted using sterile techniques and in accordance with the guidelines of the University of Toronto Animal Care Committee and the Canadian Animal Care Council. SKOV3 cells were maintained in RPMI 1640 medium supplemented with 10% (v/v) heat-inactivated fetal bovine serum and 1% (v/v) penicillin–streptomycin (100 U/ml penicillin G and 100 mg/ml streptomycin). Cells were allowed to grow in a monolayer in a tissue culture flask incubated at 37 °C, gassed with 5% CO_2 and held at 90% relative humidity. Mice were injected IP with 1×10^7 SKOV3 cells suspended in 300 μl serum-free RPMI 1640 medium. Fourteen days post-inoculation, mice ($n = 4$ per group) were injected IP under sterile conditions with $PoLi_{gel}$–LA–DTX (total DTX doses of 19.2 mg/kg or 28.8 mg/kg) blend or 50 μl sterile saline solution. All injections were done in the lower left quadrant, with an injection depth of 1 cm using a 25-gauge needle. The 28.8 mg/kg dose was chosen due to clinical relevance, while a lower dose of 19.2 mg/kg, administered via 20 μl of $PoLi_{gel}$–LA–DTX blend, was employed to examine the occurrence of a dose-dependent response. Animals were sacrificed 14 days after treatment initiation, and tumors were collected and weighed for tumor burden assessment. Body condition of mice due to tumor burden progression was monitored daily using the 'body conditioning scoring' system described elsewhere (Ullman-Cullere and Foltz, 1999). Animals were housed under sterile conditions in microisolator cages, fed standard chow diet with water ad libitum and maintained on an automatic 12 h light cycle at 22–24 °C.

2.10. HPLC analysis

An Agilent Series 1100 HPLC (Agilent Technologies, Canada) equipped with a Waters 4.6 mm × 250 mm column (XTerra® MS C_{18}, 5 μm particle size) and Waters 3.9 × 20 mm guard column (XTerra® MS C_{18}, 5 μm particle size), Waters Dual Absorbance Detector 2487 (Waters, USA) and ChemStation software (Agilent Technologies, Canada) was used for analysis. The wavelength of detection used for DTX was 227 nm. For plasma and tissue samples a mobile phase of 60% 0.01 M PBS (pH 10) and 40% acetonitrile was used (DTX retention time of 40 min). For *in vitro* release samples a mobile phase of 52% H_2O and 48% acetonitrile was used (DTX retention time of 11 min). All samples were run at a flow rate of 1 ml/min with an injection volume of 20 μl per sample. An internal standard of PTX (10 μg/ml) was used for all HPLC analysis. For the extraction of DTX from *in vitro* release and plasma samples, 300 μl of sample was added to a vial containing PTX standard. The contents were vortexed for 5 min and then 5 ml tert-butyl methyl ester was added followed by 10 min of additional vortexing. The solution was then centrifuged (Centrifuge 5804R, Eppendorf, Germany) at 4000 rpm for 15 min. The organic layer was transferred to a new vial followed by drying under nitrogen. The dried sample was then re-suspended in 300 μl of mobile phase and analyzed by HPLC. The extraction efficiency of DTX from *in vitro* release and plasma samples was greater than 90%. For the extraction of DTX from tissue samples, distilled deionized water was added at a ratio of 4 ml per gram of tissue. The sample was then homogenized (100 Sonic Dismembrator, Fisher Scientific, Canada) and added to a vial containing PTX standard. The DTX extraction procedure was similar to that described above. The extraction efficiency of DTX from tissues and blend formulation samples was greater than 80%. The limit of detection for DTX was 20.0 ng/ml for all samples.

2.11. Statistical data analysis

All results were obtained from data groups of $n \geq 3$ and are expressed as mean ± standard error. Statistical analyses were performed using Statistical Package for the Social Sciences Version 16.0 (SPSS Inc., USA). A two-sample *t*-test was used to measure statistical significance between pairs of results. For statistical analyses among three or more groups, one-way analysis of variance (ANOVA) was used and subsequent multiple comparisons with Bonferroni correction was performed if any statistical significance was detected by the ANOVA *F*-test. A p-value < 0.05 was considered to be significant.

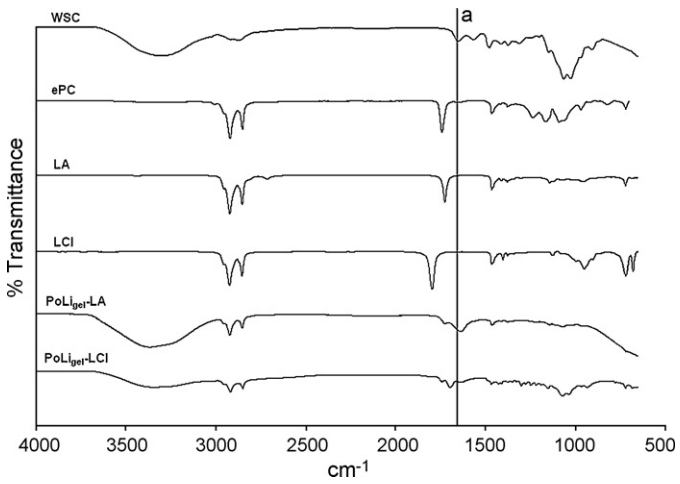

Fig. 1. FTIR spectra of water-soluble chitosan (WSC), egg phosphatidylcholine (ePC), lauric aldehyde (LA), lauric chloride (LCl), PoLi$_{gel}$–LA blend, and PoLi$_{gel}$–LCL blend.

3. Results and discussion

3.1. PoLi$_{gel}$ blend characterization—lauric aldehyde vs. lauric chloride

In order to establish the interactions that stabilize the PoLi$_{gel}$ blends, FTIR spectra were collected. The spectra of each blend and their individual components were analyzed for characteristic peaks (Fig. 1). In agreement with other reports, FTIR analysis confirmed favorable interactions between chitosan and ePC with a shift of the primary amine group of WSC from 1564 cm^{-1} (Fig. 1, line a) to around 1575 cm^{-1} with the addition of ePC (Grant et al., 2005; Cho et al., 2006). Furthermore, the absence of a defined peak at 1800 cm^{-1} (CClO group in LCl) in the PoLi$_{gel}$–LCl blend spectra and at 1725 cm^{-1} (CHO group LA) in the PoLi$_{gel}$–LA blend spectra, as seen in Fig. 1, indicates that LCl and LA groups interacted with the primary amine groups of WSC (peak at 1564 cm^{-1}) and/or groups within ePC (P=O at 1226 cm^{-1}). Previous work by Grant et al. outlines in detail these stabilizing interactions for various PoLi$_{gel}$–LCl blends (Grant et al., 2008), with similar interactions seen here for the PoLi$_{gel}$–LA blend.

It has been shown that using C12–LCl as compared to C10, C14 and C16 LCls, results in the most stable injectable chitosan–phospholipid blend formulation; however, a low pH profile was observed *in vitro* (Grant et al., 2008). It has been reported in different studies that C12 alkyl chains grafted onto the chitosan backbone lead to formation of stable gels (Iversen et al., 1997; Ramos et al., 2003). Rinaudo et al. have shown from a series of alkylated chitosan derivatives that the C12 alkyl chain was the optimal chain length for forming a stable gel (Rinaudo et al., 2005). In addition, in a recent study by our group, De Souza et al. demonstrated superior biocompatibility of the PoLi$_{gel}$ blend both *in vitro* and *in vivo* when C12–LCl was replaced by C12–LA (De Souza et al., 2009). To confirm the advantage of using C12–LA over C12–LCl for preparing the PoLi$_{gel}$ blend, stability and pH testing were conducted. The effect of drug loading on stability and pH were also investigated for PoLi$_{gel}$–LA blend. The stability of the PoLi$_{gel}$–LA, PoLi$_{gel}$–LA–DTX and PoLi$_{gel}$–LCl blends was assessed by turbidity measurements in 0.01 M PBS (pH 7.4) containing 2 mg/ml lysozyme at 37 °C over a 2-week period (Fig. 2A). It has been shown that chitosan is degraded by various hydrolytic enzymes including chitosanase, chitinases, cellulase, protease, lipase and lysozyme (Fukamizo and Brzezinski, 1997). Lysozyme solutions have been used in various reports for studying the *in vitro* biodegradation (i.e. stability) of chitosan-based systems (Hirano et al., 1989; Lee et al., 1995; Onishi and Machida, 1999; Mao et al., 2003; Freier et al., 2005; Ma et al., 2008). The PoLi$_{gel}$–LCl blend disintegrated within 3 h following injection into the lysozyme solution as can be seen from the high absorbance values in Fig. 2A. However, the PoLi$_{gel}$–LA and PoLi$_{gel}$–LA–DTX blends were stable over the 2-week incubation period as indicated by negligible absorbance values (Fig. 2A). A significant decrease in the pH of 0.01 M PBS solution from 7.4 to approximately 2.75 within 3 h of incubation was seen for the PoLi$_{gel}$–LCl blend (Fig. 2B). This low pH was maintained over the 2-week observation period. The decrease in pH can be attributed to the formation of the acidic by-products of LCl during the reaction with water and/or WSC as reported in our previous work (Grant et al., 2008), and to the low stability of the PoLi$_{gel}$–LCl formulation as confirmed by turbidity measurements. In contrast, the pH profiles of the PoLi$_{gel}$–LA and PoLi$_{gel}$–LA–DTX blends were maintained close to neutral pH over 2 weeks ($p > 0.05$).

3.2. PoLi$_{gel}$–LA blend morphology

Confocal laser scanning microscopy was used to gain insight into the molecular organization of the materials within the PoLi$_{gel}$–LA blend. The red regions shown in Fig. 3A represent the WSC component and the green regions in Fig. 3B correspond to the phospholipid (ePC) component. Fig. 3C shows the overlay of the phospholipid and WSC regions, indicating areas of colocalization between the WSC and ePC. The colocalization between the WSC and phospholipid is

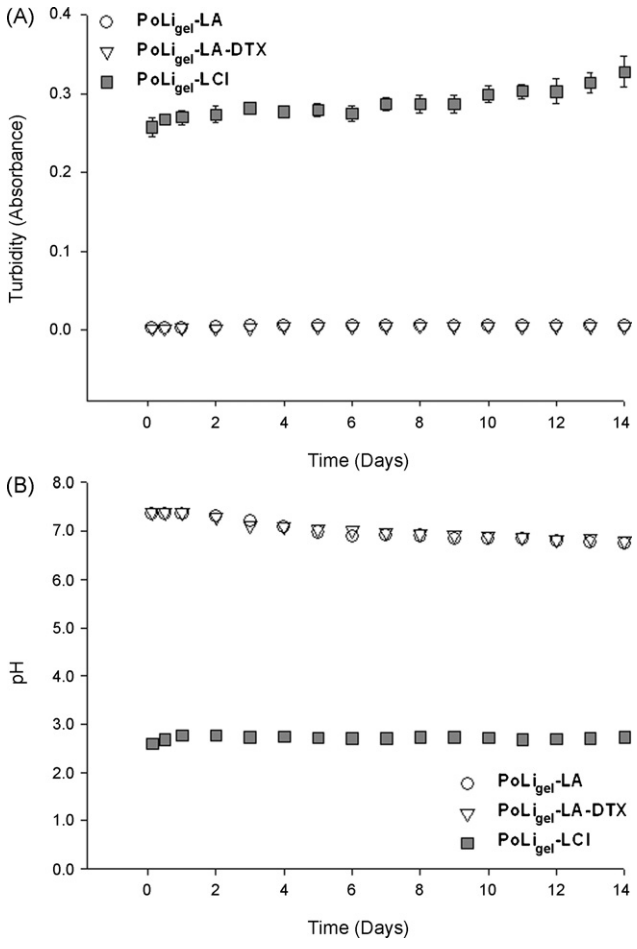

Fig. 2. *In vitro* characterization of the stability and pH profiles of PoLi$_{gel}$ blends. (A) Turbidity measured as absorbance of 0.01 M PBS (pH 7.4) solution containing PoLi$_{gel}$ blend, as a function of time. (B) pH values of 0.01 M PBS (pH 7.4) solution containing PoLi$_{gel}$ blend, as a function of time. Error bars are expressed as standard error ($n = 6$).

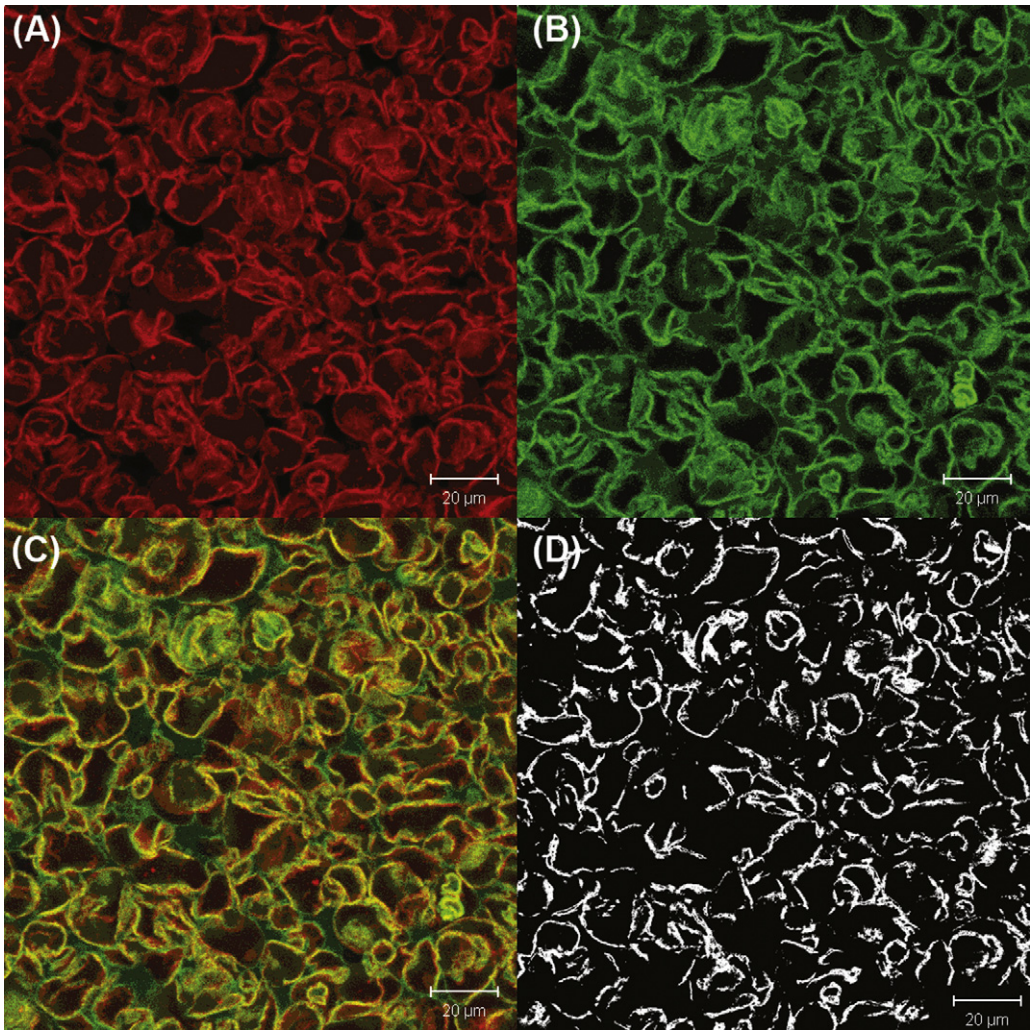

Fig. 3. Confocal laser scanning fluorescence microscopy images of the $PoLi_{gel}$–LA blend. (A) WSC regions, (B) ePC regions, (C) overlay of the WSC and ePC regions and (D) colocalization of WSC and ePC regions. The scale bar in each image represents 20 μm.

critical in stabilization of the blend as reported previously (Grant et al., 2008). In order to quantify the extent to which WSC–ePC colocalized, a map was generated (Fig. 3D). WSC–ePC was found to colocalize in regions surrounding a mean object area of 11.2 μm^2 (i.e. yellow regions). The mean gray value within the colocalization map (i.e. amount of bright pixels relative to the background) was 31%. The colocalization coefficients M1 and M2, which represent the contribution of the ePC (green fluorescent signal) and WSC (red fluorescent signal) to the colocalized areas, were 46% and 43%, respectively. As summarized in Table 1, the $PoLi_{gel}$–LA blend showed higher mean object area and colocalization coefficients (M1 and M2) and comparable mean gray value to the $PoLi_{gel}$–LCl blend. As noted elsewhere, higher mean object area, colocalization coefficients and mean gray value are often indicative of enhanced stability (Grant et al., 2008).

3.3. *$PoLi_{gel}$ blend rheological analysis*

The rheological properties of the injectable blends were assessed by viscosity measurements using steady shear tests (Fig. 4). It has been reported that low viscosity injectable systems may fail to provide a delayed drug release profile while high viscosity injectables may be difficult to administer (Hatefi and Amsden, 2002). It has been established that needles of 22-gauge and above are acceptable for injection of a drug formulation; otherwise, pumps and other systems need to be utilized (Packhaeuser et al., 2004). The blends tested here were injectable through a 22-gauge needle. At low shear rate all the blends displayed Newtonian flow, and as the shear rate increased a shear-thinning (non-Newtonian) trend was observed. The $PoLi_{gel}$–LCl blend had a faster onset of shear-thinning than the $PoLi_{gel}$–LA blend (Fig. 4). During rheological testing the $PoLi_{gel}$–LCl

Table 1
Colocalization analysis of the WSC and ePC regions within the $PoLi_{gel}$–LA and $PoLi_{gel}$–LCl blends using confocal microscopy.

Blend	Mean object area (μm^2)[a]	M1 (ePC)[b]	M2 (WSC)[b]	Mean gray value[c]	Reference
$PoLi_{gel}$–LA	11.2	46	43	31	–
$PoLi_{gel}$–LCL	8.5	42	39	30	Grant et al. (2008)

[a] Mean object areas represent the average area surrounded by colocalized WSC and ePC in the colocalization map (Fig. 3D).
[b] M1 and M2 represent the percentage of ePC (green) and WSC (red) fluorescence signals in the colocalized area relative to the total ePC and WSC fluorescence signals, respectively (Fig. 3C).
[c] Mean gray values represent the amount of bright pixels detected in the WSC–ePC colocalization map (Fig. 3D).

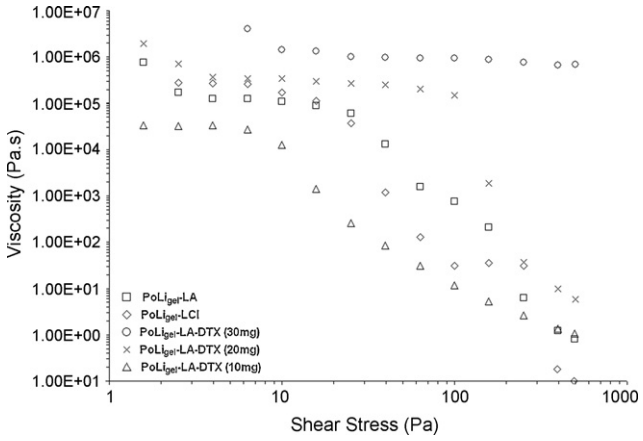

Fig. 4. Viscosity (η) as a function of shear stress (σ) for different PoLi$_{gel}$ blends characterized by a stress-controlled rheometer with a 4 cm cone and 2° angle plate geometry attachment at room temperature.

blend at high shear rates separated, however, this was not observed for the PoLi$_{gel}$–LA blend. This further illustrates the higher stability of the PoLi$_{gel}$–LA blend compared to the PoLi$_{gel}$–LCl blend. The effect of initial drug loading on rheology of the PoLi$_{gel}$–LA blend was also assessed. As shown in Fig. 4, an increase in the drug loading level resulted in an increase in the viscosity of the formulation. Furthermore, the onset of shear-thinning was seen at higher shear rates as the drug loading level increased. Based on stability assessment, pH profile, colocalization data and rheological measurements, the PoLi$_{gel}$–LA blend showed superior stability properties in comparison to the PoLi$_{gel}$–LCl blend. As such, the PoLi$_{gel}$–LA blend was further characterized as a delivery system for DTX.

3.4. In vitro DTX release

As shown in Fig. 5, the *in vitro* release of DTX from the PoLi$_{gel}$–LA blend as a function of initial drug loading was evaluated in buffer containing lysozyme and albumin. As mentioned previously, lysozyme is known to degrade chitosan. We have previously shown that evaluation of *in vitro* drug release in PBS buffer (0.01 M pH 7.4) containing 2 mg/ml lysozyme accurately models drug release in ascites, a fluid found in high abundance in the peritoneal cavity of ovarian cancer patients (Lim Soo et al., 2008). Ascites (pH ~ 7.4–7.8) is composed of various proteins including serum albumin (Adam and Adam, 2004) and taxane drugs such as DTX have been shown to have high affinity for albumin (Urien et al., 1996). For these reasons, lysozyme and albumin were added to the release media to better model physiological conditions.

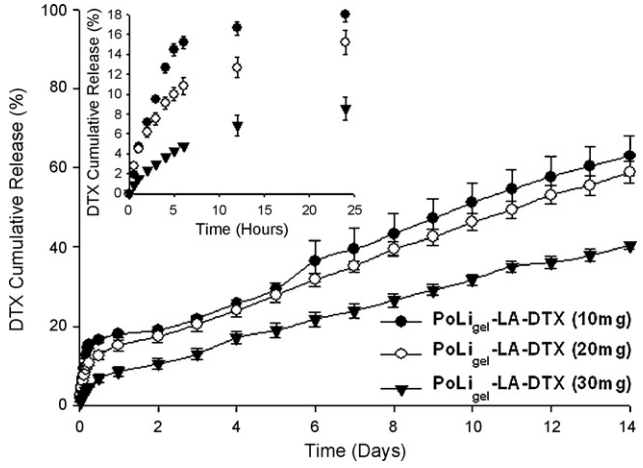

Fig. 5. *In vitro* release of DTX from PoLi$_{gel}$–LA blends as a function of initial DTX loading level in 0.01 M PBS (pH 7.4) with 2 mg/ml lysozyme and 40 mg/ml albumin at 37 °C over a 2-week period. Error bars are expressed as standard error ($n = 3$).

A biphasic release profile was obtained for DTX over the 2-week study period, characterized by a more rapid release phase during the initial 24 h (i.e. in terms of % released per day) and a sustained, slower drug release phase for the remainder of the 14-day period. The initial higher release phase can be attributed to drug associated with the surface of the blend. The sustained phase can be attributed to the DTX that has partitioned into the hydrophobic regions (i.e. phospholipid and LA) within the blend. During the initial 24 h period, 8–17% of total DTX loaded in the PoLi$_{gel}$–LA blends was released. Following the initial 24 h, a sustained release rate of $3.7 \pm 1.9\%$, $3.4 \pm 0.6\%$ and $2.4 \pm 0.7\%$ of DTX per day was seen from the 10, 20 and 30 mg DTX loaded PoLi$_{gel}$–LA blends, respectively. The release rate of DTX from the PoLi$_{gel}$–LA blend was concentration-dependent, with a lower drug loading level resulting in more drug released within the first 24 h (i.e. 17%) followed by a higher rate of sustained drug release during the second phase (i.e. $3.7 \pm 1.9\%$), in comparison to the formulations with higher drug loading levels. This may be attributed to the rheological properties of the formulations. As shown in Fig. 4, the rheological properties increased by approximately two orders of magnitude (i.e. $\eta \sim 3 \times 10^4$ to $\eta \sim 6 \times 10^6$ Pa s) when the drug loading level increased from 10 to 30 mg. In general, blend viscosity can increase when there are greater interactions between the different molecules that comprise the formulation, including molecular entanglements, physical interactions (i.e. hydrophobic, van der Waals and hydrogen bonding) and cross-linking (Grant et al., 2008). These types of interactions can consequently entrap the drug and therefore reduce the rate of drug release.

3.5. In vivo DTX distribution

As shown in Fig. 6A, constant plasma drug levels, with an average of 56.2 ± 9.3 ng/ml DTX, were detected over the 2-week study period ($4.4 \pm 0.7\%$ DTX per day). The sustained *in vivo* DTX levels were on par with the observed sustained *in vitro* release ($2.4 \pm 0.7\%$ DTX per day). Tissue drug concentrations were also examined (Fig. 6B). Levels were significantly higher ($p < 0.05$) in the peritoneal muscle and intestines when compared to liver, spleen, kidneys and heart. The average drug accumulation per day in the various organs or tissues, over the 2-week study period, was as follows: peritoneal muscle ($13.1 \times 10^3 \pm 3.4 \times 10^3$ ng/g), intestines (1226.9 ± 446.2 ng/g), liver (522.7 ± 85.6 ng/g), spleen (461.8 ± 58.5 ng/g), kidneys (239.4 ± 57.2 ng/g) and heart (201.5 ± 23.2 ng/g). Constant drug levels were seen in all tissues over 2 weeks ($p > 0.05$) with the exception of the peritoneal muscle on day 7 ($p < 0.05$).

DTX concentrations in the peritoneal muscle and intestines were 234 and 22 times higher than concentrations found in plasma, respectively. Comparable to our findings, Marchettini et al. also detected highest drug concentrations within the abdominal wall and colon of male Sprague–Dawley rats following bolus IP administration of Taxotere® (Marchettini et al., 2002). This is explained by the fact that IP administration leads to tissue drug uptake not only via the systemic circulation, as would be the case after IV administration, but also directly from the peritoneal cavity (Shimada et al., 2005). Our localized delivery approach leads to high local drug concentrations and much lower systemic exposure which should theoretically result in reduced toxicity to healthy tissues such as the bone marrow and greater efficacy than IV chemotherapy (de Bree et al., 2006). High concentrations in the peritoneal region, especially in the peritoneal muscle, suggest the application of this formulation in the treatment of cancers originating in the peritoneal cavity

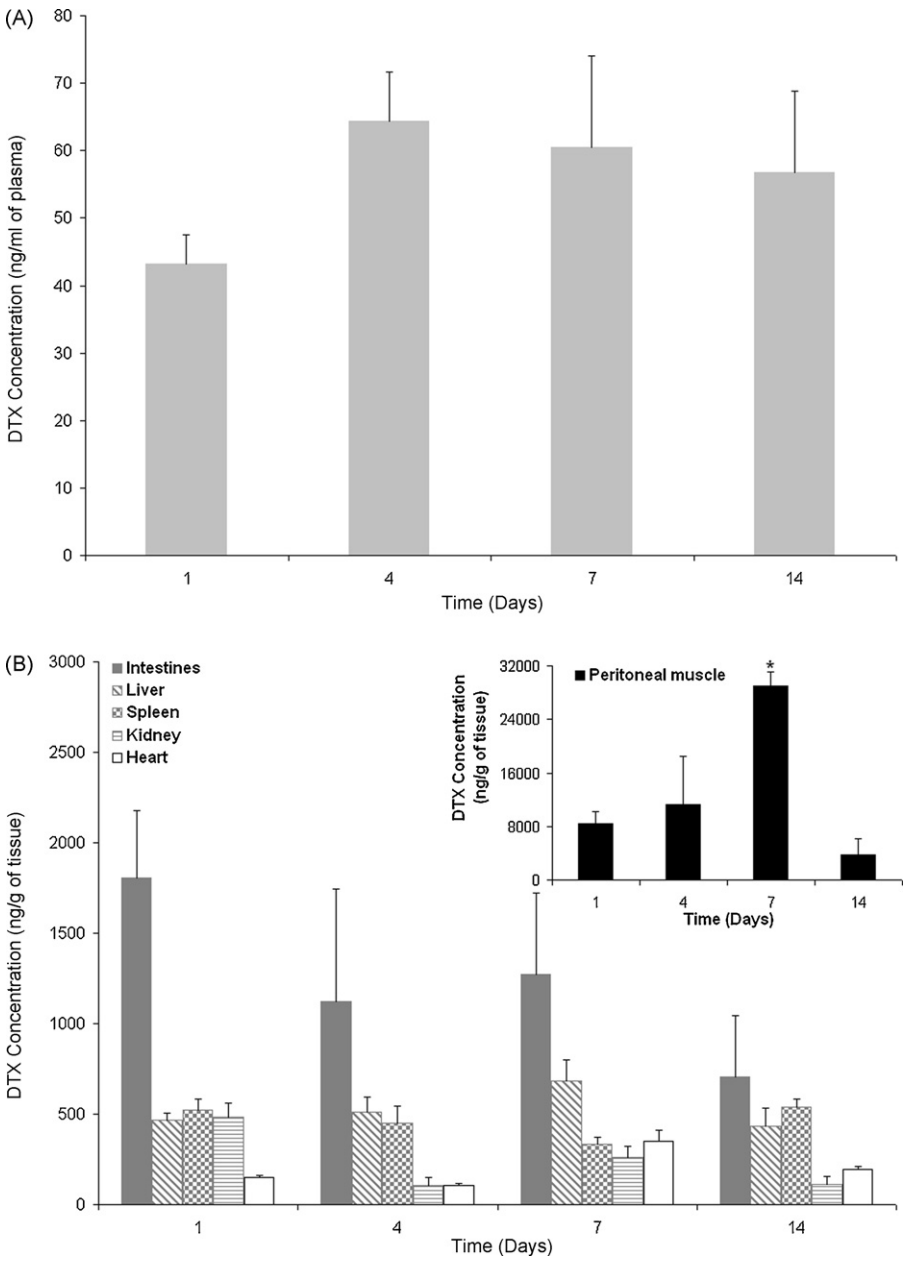

Fig. 6. *In vivo* DTX distribution following IP administration of $PoLi_{gel}$–LA–DTX blend in healthy female CD-1 mice (total DTX dose: 28.8 mg/kg). (A) *In vivo* plasma concentrations. (B) Biodistribution of DTX in various tissues (liver, spleen, kidney, heart, peritoneal muscle, and intestines). Error bars are expressed as standard error ($n = 6$). No significant differences in plasma or tissue concentrations were seen between samples obtained from treated mice on days 1, 4, 7 and 14 with the exception of the peritoneal muscle on day 7.

and those presenting peritoneal dissemination, such as gastrointestinal, ovarian, colorectal, pancreatic and others (Flessner, 2007). In these cases, metastatic lesions form along the peritoneal lining. Damage to the lining due to surgical removal of the lesions is known to encourage further peritoneal metastasis; thus, the high drug levels in the peritoneal muscle seen in this study present an attractive therapeutic alternative to surgery (Oosterling et al., 2005).

Consistent with biocompatibility studies performed using the drug-free $PoLi_{gel}$–LA blend, loading the formulation with DTX does not alter its biocompatibility (De Souza et al., 2009). According to visual observation, the high drug levels found in the intestines did not lead to intestinal toxicity (i.e. no signs of paralytic ileus). In fact, clinical observation has noted the presence of a rich capillary network with high flow rates which protects the proliferative intestinal tissue upon IP chemotherapeutic delivery (Howell, 2008). Throughout the study period no signs of toxicity were observed, as the animals did not display weight loss, signs of immobility, anorexia, dehydration, or peritonitis. At all time points, the formulation was found free of fibrous encapsulation, which would be indicative of a foreign body response. ALT levels in both control mice and those injected with the formulation (25 ± 8 and 17 ± 4 U/l, respectively) remained well below 200 U/l, levels which are indicative of hepatotoxicity in mice (Clement and Williams, 2005; Masubuchi et al., 2005; Wang et al., 2007). As it is plausible that introduction of foreign material into the body can result in immune response and tissue injury, resulting in the activation of an inflammatory reaction (Anderson, 2001; Pavithra and Doble, 2008), we monitored circulating levels of IL-6, a systemic pro-inflammatory mediator. IL-6 plasma concentrations of 53 ± 9 and 27 ± 5 pg/ml were seen in treated and control animals, respectively ($p < 0.05$). Despite the

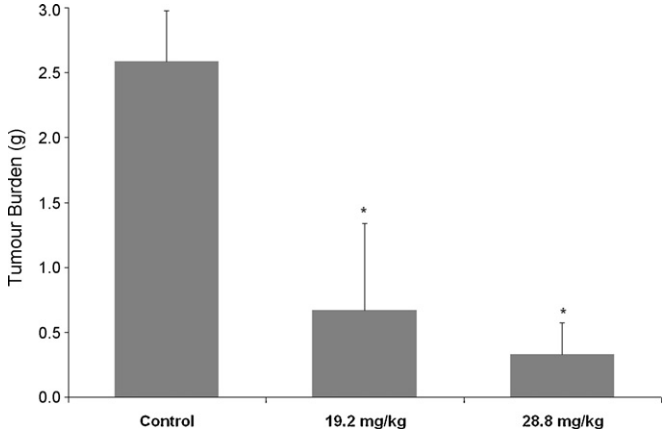

Fig. 7. PoLi$_{gel}$–LA–DTX blend anti-tumor efficacy in SKOV3 ovarian cancer xenograft model. Human ovarian tumors were induced by SKOV3 cell inoculation in female CD-1 nu/nu mice. Treatment with PoLi$_{gel}$–LA–DTX blends (total DTX doses: 28.8 and 19.2 mg/kg) was initiated 14 days post-SKOV3 inoculation, with 50 μl injected sterile saline solution as control. Significant difference was found between the treatment groups and control, $p < 0.05$. Error bars are expressed as standard error ($n = 4$).

slight increase in IL-6 values seen in treated mice, these levels are still within the normal reported range for healthy CD-1 mice and are greatly below levels reported to be indicative of significant inflammation (Bobrowski et al., 2005). For example, CD-1 mice with peritonitis typically have serum IL-6 levels in the range of 10–15 ng/ml (Walley et al., 1997). Overall, these results indicate that PoLi$_{gel}$–LA–DTX blend does not induce significant local toxicity or systemic inflammation.

3.6. Anti-tumor efficacy

The ability of PoLi$_{gel}$–LA–DTX blend to inhibit tumor growth was assessed in a SKOV3 xenograft model of human ovarian adenocarcinoma. As shown in Fig. 7, both doses of PoLi$_{gel}$–LA–DTX blend used demonstrated anti-tumor efficacy when compared to control animals ($p < 0.05$). A tumor burden reduction of $87.3 \pm 9.3\%$ was achieved with the 28.8 mg/kg dose. A $74.1 \pm 25.9\%$ tumor burden reduction was achieved at a does of 19.2 mg/kg, a dose that is lower than the recommended IP dose for ovarian cancer patients in clinical trials (Morgan et al., 2003). These results show that even a lower dose of DTX delivered in a sustained and localized manner via the PoLi$_{gel}$–LA blend results in significant tumor inhibition. It should be noted that since the PoLi$_{gel}$–LA blend provides sustained release of DTX over a prolonged period of time in a localized environment, the therapeutically relevant dose for treatment of ovarian cancer may differ from that required for bolus IP administration of this agent.

It has been shown that frequent, low-dose chemotherapy, referred to as 'metronomic' chemotherapy, provides superior anti-tumor effects and clinical efficacy over the traditional maximum tolerated dose (MTD) approach (Lennernas et al., 2004). Previously developed chitosan–phospholipid film implants capable of continuous PTX delivery have demonstrated excellent efficacy against SKOV3 xenograft tumor models when compared to that achieved by intermittent MTD regimens (Vassileva et al., 2007, 2008b). In these studies, greater efficacy of sustained therapy was attributed to a decrease in tumor cell repopulation and a lack of drug resistance gene up-regulation (Ho et al., 2007; Vassileva et al., 2008a). Since DTX is a semi-synthetic analogue of PTX, it is plausible that these similar mechanisms contribute to the high efficacy seen in this study; however, further studies are needed to explore possible mechanisms. The PoLi$_{gel}$–LA–DTX blend has the potential to provide low toxicity and high efficacy associated with continuous, low-dose chemotherapy, as shown by this pilot study of efficacy. Future studies will focus on comparing the efficacy of frequent low doses of DTX, provided by PoLi$_{gel}$–LA–DTX blend, to Taxotere® administered in a maximum tolerated dose regimen.

4. Conclusions

To our knowledge, this is the first report of a delivery system that provides localized and sustained delivery of DTX following IP administration. The injectable blend was found to result in sustained plasma concentrations of DTX and constant levels of drug exposure in the peritoneal cavity of healthy mice over the 2-week period, with no signs of toxicity or inflammation. Furthermore, the injectable blend showed significant tumor inhibition in a murine xenograft model of human ovarian adenocarcinoma. This localized delivery system has excellent potential for sustained IP treatment of cancers, such as ovarian, that reside in the peritoneal cavity and may be utilized for delivery of other anti-cancer drugs as well.

Acknowledgments

The authors thank J. Zhang for assisting with HPLC analysis and Dr. D.F. James and R. Grau for assistance with rheological measurements. This research was funded by Natural Sciences and Engineering Research Council (NSERC) and the Canadian Cancer Society (CCS). P. Zahedi and R. De Souza are grateful to NSERC for Industrial Postgraduate Scholarships.

References

Adam, R.A., Adam, Y.G., 2004. Malignant ascites: past, present, and future. J. Am. Coll. Surg. 198, 999–1011.
Ali, S.M., Hoemann, M.Z., Aube, J., Georg, G.I., Mitscher, L.A., Jayasinghe, L.R., 1997. Butitaxel analogues: synthesis and structure–activity relationships. J. Med. Chem. 40, 236–241.
Anderson, J.M., 2001. Biological responses to materials. Annu. Rev. Mater. Res. 31, 81–110.
Angelova, N., Hunkeler, D., 1999. Rationalizing the design of polymeric biomaterials. Trends Biotechnol. 17, 409–421.
Bobrowski, W.F., McDuffie, J.E., Sobocinski, G., Chupka, J., Olle, E., Bowman, A., Albassam, M., 2005. Comparative methods for multiplex analysis of cytokine protein expression in plasma of lipopolysaccharide-treated mice. Cytokine 32, 194–198.
Cho, J., Grant, J., Piquette-Miller, M., Allen, C., 2006. Synthesis and physicochemical and dynamic mechanical properties of a water-soluble chitosan derivative as a biomaterial. Biomacromolecules 7, 3548–13548.
Clarke, S.J., Rivory, L.P., 1999. Clinical pharmacokinetics of docetaxel. Clin. Pharmacokinet. 36, 99–114.
Clement, Y.N., Williams, A.F., 2005. Protection against paracetamol-induced hepatic injury by prazosin pre-treatment in CD-1 mice. Mutat. Res. 579, 182–188.
Crown, J., O'Leary, M., 2000. The taxanes: an update. Lancet 355, 1176–1178.
de Bree, E., Theodoropoulos, P.A., Rosing, H., Michalakis, J., Romanos, J., Beijnen, J.H., Tsiftsis, D.D., 2006. Treatment of ovarian cancer using intraperitoneal chemotherapy with taxanes: from laboratory bench to bedside. Cancer Treat. Rev. 32, 471–482.
De Souza, R., Zahedi, P., Allen, C., Piquette-Miller, M., 2009. Biocompatibility of injectable chitosan–phospholipid implant systems. Biomaterials, 003, doi:10.1016/j.biomaterials.2009.04.
Dhanikula, A.B., Panchagnula, R., 1999. Localized paclitaxel delivery. Int. J. Pharm. 183, 85–100.
Engels, F.K., Mathot, R.A.A., Verweij, J., 2007. Alternative drug formulations of docetaxel: a review. Anti-Cancer Drugs 18, 95–103.
Flessner, M.F., 2007. Intraperitoneal Drug Therapy: Physical and Biological Principles. Springer, New York, US.
Freier, T., Koh, H.S., Kazazian, K., Shoichet, M.S., 2005. Controlling cell adhesion and degradation of chitosan films by N-acetylation. Biomaterials 26, 5872–5878.
Fukamizo, T., Brzezinski, R., 1997. Chitosanase from *Streptomyces* sp. strain N174: a comparative review of its structure and function. Biochem. Cell. Biol. 75, 687–696.
Fulzele, S.V., Satturwar, P.M., Dorle, A.K., 2003. Study of the biodegradation and in vivo biocompatibility of novel biomaterials. Eur. J. Pharm. Sci. 20, 53–61.
Fung, L.K., Saltzman, W.M., 1997. Polymeric implants for cancer chemotherapy. Adv. Drug. Deliver. Rev. 26, 209–230.
Gligorov, J., Lotz, J.P., 2004. Preclinical pharmacology of the taxanes: implications of the differences. Oncologist 9, 3–8.
Gottesman, M.M., 2002. Mechanisms of cancer drug resistance. Annu. Rev. Med. 53, 615–627.
Grant, J., Blicker, M., Piquette-Miller, M., Allen, C., 2005. Hybrid films from blends of chitosan and egg phosphatidylcholine for localized delivery of paclitaxel. J. Pharm. Sci. 94, 1512–1527.

Grant, J., Lee, H., Lim Soo, P., Cho, J., Piquette-Miller, M., Allen, C., 2008. Influence of molecular organization and interactions on drug release for an injectable polymer–lipid blend. Int. J. Pharm. 360, 83–90.
Grant, J., Tomba, J.P., Lee, H., Allen, C., 2007. Relationship between composition and properties for stable chitosan films containing lipid microdomains. J. Appl. Polym. Sci. 103, 3453–3460.
Grayson, A.C.R., Voskerician, G., Lynn, A., Anderson, J.M., Cima, M.J., Langer, R., 2004. Differential degradation rates in vivo and in vitro of biocompatible poly(lactic acid) and poly(glycolic acid) homo- and co-polymers for a polymeric drug-delivery microchip. J. Biomater. Sci. Polym. Ed. 15, 1281–1304.
Hatefi, A., Amsden, B., 2002. Biodegradable injectable in situ forming drug delivery systems. J. Control. Release 80, 9–28.
Hennenfent, K.L., Govindan, R., 2006. Novel formulations of taxanes: a review. Old wine in a new bottle? Ann. Oncol. 17, 735–749.
Hickey, T., Kreutzer, D., Burgess, D.J., Moussy, F., 2002. In vivo evaluation of a dexamethasone/PLGA microsphere system designed to suppress the inflammatory tissue response to implantable medical devices. J. Biomed. Mater. Res. 61, 180–187.
Hirano, S., Tsuchida, H., Nagao, N., 1989. N-acetylation in chitosan and the rate of its enzymic-hydrolysis. Biomaterials 10, 574–576.
Ho, E.A., Soo, P.L., Allen, C., Piquette-Miller, M., 2007. Impact of intraperitoneal, sustained delivery of paclitaxel on the expression of P-glycoprotein in ovarian tumors. J. Control. Release 117, 20–27.
Ho, E.A., Vassileva, V., Allen, C., Piquette-Miller, M., 2005. In vitro and in vivo characterization of a novel biocompatible polymer–lipid implant system for the sustained delivery of paclitaxel. J. Control. Release 104, 181–191.
Howell, S.B., 2008. Pharmacologic principles of intraperitoneal chemotherapy for the treatment of ovarian cancer. Int. J. Gynecol. Cancer 18, 20–25.
Iversen, C., Kjoniksen, A.L., Nystrom, B., Nakken, T., Palmgren, O., Tande, T., 1997. Linear and nonlinear rheological responses in aqueous systems of hydrophobically modified chitosan and its unmodified analogue. Polym. Bull. 39, 747–754.
Kerbel, R.S., 2005. Inhibition of tumor angiogenesis as a strategy to circumvent acquired resistance to anti-cancer therapeutic agents. Bioessays 13, 31–36.
Kerbel, R.S., Kamen, B.A., 2004. The anti-angiogenic basis of metronomic chemotherapy. Nat. Rev. Cancer 4, 423–436.
Lee, K.Y., Ha, W.S., Park, W.H., 1995. Blood compatibility and biodegradability of partially N-acylated chitosan derivatives. Biomaterials 16, 1211–1216.
Lennernas, B., Albertsson, P., Damber, J.E., Norrby, K., 2004. Antiangiogenic effect of metronomic paclitaxel treatment in prostate cancer and non-tumor tissue in the same animals: a quantitative study. APMIS 112, 201–209.
Lim, S.H., Hudson, S.M., 2004. Synthesis and antimicrobial activity of a water-soluble chitosan derivative with a fiber-reactive group. Carbohydr. Res. 339, 313–319.
Lim Soo, P., Cho, J., Grant, J., Ho, E., Piquette-Miller, M., Allen, C., 2008. Drug release mechanism of paclitaxel from a chitosan–lipid implant system: effect of swelling, degradation and morphology. Eur. J. Pharm. Biopharm. 69, 149–157.
Lowenthal, R.M., Eaton, K., 1996. Toxicity of chemotherapy. Hematol. Oncol. Clin. North Am. 10, 967–990.
Ma, G.P., Yang, D.Z., Zhou, Y.S., Xiao, M., Kennedy, J.F., Nie, J., 2008. Preparation and characterization of water-soluble N-alkylated chitosan. Carbohydr. Polym. 74, 121–126.
Maenpaa, J.U., 2003. Docetaxel: promising and novel combinations in ovarian cancer. Brit. J. Cancer 89, S29–S34.
Mao, J.S., Liu, H.F., Yin, Y.J., Yao, K.D., 2003. The properties of chitosan–gelatin membranes and scaffolds modified with hyaluronic acid by different methods. Biomaterials 24, 1621–1629.
Marchettini, P., Stuart, O.A., Mohamed, F., Yoo, D., Sugarbaker, P.H., 2002. Docetaxel: pharmacokinetics and tissue levels after intraperitoneal and intravenous administration in a rat model. Cancer Chemoth. Pharm. 49, 499–503.
Masubuchi, Y., Suda, C., Horie, T., 2005. Involvement of mitochondrial permeability transition in acetaminophen-induced liver injury in mice. J. Hepatol. 42, 110–116.
Morgan, R.J., Doroshow, J.H., Synold, T., Lim, D., Shibata, S., Margolin, K., Schwarz, R., Leong, L., Somlo, G., Twardowski, P., Yen, Y., Chow, W., Lin, P., Paz, B., Chu, D., Frankel, P., Stalter, S., 2003. Phase I trial of intraperitoneal docetaxel in the treatment of advanced malignancies primarily confined to the peritoneal cavity: dose-limiting toxicity and pharmacokinetics. Clin. Cancer Res. 9, 5896–5901.
Onishi, H., Machida, Y., 1999. Biodegradation and distribution of water-soluble chitosan in mice. Biomaterials 20, 175–182.
Oosterling, S.J., van der Bij, G.J., van Egmond, M., van der Sijp, J.R.M., 2005. Surgical trauma and peritoneal recurrence of colorectal carcinoma. Eur. J. Surg. Oncol. 31, 29–37.
Packhaeuser, C.B., Schnieders, J., Oster, C.G., Kissel, T., 2004. In situ forming parenteral drug delivery systems: an overview. Eur. J. Pharm. Biopharm. 58, 445–455.
Panchagnula, R., 1998. Pharmaceutical aspects of paclitaxel. Int. J. Pharm. 172, 1–15.
Parveen, S., Sahoo, S.K., 2008. Polymeric nanoparticles for cancer therapy. J. Drug. Target. 16, 108–123.
Pavithra, D., Doble, M., 2008. Biofilm formation, bacterial adhesion and host response on polymeric implants—issues and prevention. Biomed. Mater. 3, 1–13.
Pillai, O., Panchagnula, R., 2001. Polymers in drug delivery. Curr. Opin. Chem. Biol. 5, 447–451.
Ramos, V.M., Rodriguez, N.M., Rodriguez, M.S., Heras, A., Agullo, E., 2003. Modified chitosan carrying phosphonic and alkyl groups. Carbohydr. Polym. 51, 425–429.
Rinaudo, M., Auzely, R., Vallin, C., Mullagaliev, I., 2005. Specific interactions in modified chitosan systems. Biomacromolecules 6, 2396–2407.
Shimada, T., Nomura, M., Yokogawa, K., Endo, Y., Sasaki, T., Miyamoto, K., Yonemura, Y., 2005. Pharmacokinetic advantage of intraperitoneal injection of docetaxel in the treatment for peritoneal dissemination of cancer in mice. J. Pharm. Pharmacol. 57, 177–181.
Sinha, V.R., Trehan, A., 2005. Formulation, characterization, and evaluation of ketorolac tromethamine-loaded biodegradable microspheres. Drug Deliv. 12, 133–139.
Ta, H.T., Dass, C.R., Dunstan, D.E., 2008. Injectable chitosan hydrogels for localised cancer therapy. J. Control. Release 126, 205–216.
Tannock, I.F., Lee, C.M., Tunggal, J.K., Cowan, D.S.M., Egorin, M.J., 2002. Limited penetration of anticancer drugs through tumor tissue: a potential cause of resistance of solid tumors to chemotherapy. Clin. Cancer Res. 8, 878–884.
Tsai, M., Lu, Z., Wang, J., Yeh, T.K., Wientjes, M.G., Au, J.L.S., 2007. Effects of carrier on disposition and antitumor activity of intraperitoneal paclitaxel. Pharm. Res. 24, 1691–1701.
Ullman-Cullere, M.H., Foltz, C.J., 1999. Body condition scoring: a rapid and accurate method for assessing health status in mice. Lab. Anim. Sci. 49, 319–323.
Urien, S., Barre, J., Morin, C., Paccaly, A., Montay, G., Tillement, J.P., 1996. Docetaxel serum protein binding with high affinity to alpha(1)-acid glycoprotein. Invest. New Drugs 14, 147–151.
van Zuylen, L., Verweij, J., Sparreboom, A., 2001. Role of formulation vehicles in taxane pharmacology. Invest. New Drugs 19, 125–141.
Vassileva, V., Allen, C.J., Piquette-Miller, M., 2008a. Effects of sustained and intermittent paclitaxel therapy on tumor repopulation in ovarian cancer. Mol. Cancer Ther. 7, 630–637.
Vassileva, V., Grant, J., De Souza, R., Allen, C., Piquette-Miller, M., 2007. Novel biocompatible intraperitoneal drug delivery system increases tolerability and therapeutic efficacy of paclitaxel in a human ovarian cancer xenograft model. Cancer Chemoth. Pharm. 60, 907–914.
Vassileva, V., Moriyama, E.H., De Souza, R., Grant, J., Allen, C.J., Wilson, B.C., Piquette-Miller, M., 2008b. Efficacy assessment of sustained intraperitoneal paclitaxel therapy in a murine model of ovarian cancer using bioluminescent imaging. Br. J. Cancer 99, 2037–2043.
Vukelja, S.J., Anthony, S.P., Arseneau, J.C., Berman, B.S., Cunningham, C.C., Nemunaitis, J.J., Samlowski, W.E., Fowers, K.D., 2007. Phase 1 study of escalating-dose OncoGel® (ReGel®/paclitaxel) depot injection, a controlled-release formulation of paclitaxel, for local management of superficial solid tumor lesions. Anti-Cancer Drugs 18, 283–289.
Walley, K.R., Lukacs, N.W., Standiford, T.J., Strieter, R.M., Kunkel, S.L., 1997. Elevated levels of macrophage inflammatory protein 2 in severe murine peritonitis increase neutrophil recruitment and mortality. Infect. Immun. 65, 3847–3851.
Wang, H., Xu, D.X., Lv, J.W., Ning, H., Wei, W., 2007. Melatonin attenuates lipopolysaccharide (LPS)-induced apoptotic liver damage in D-galactosamine-sensitized mice. Toxicology 237, 49–57.